*Journal of Organometallic Chemistry*, 372 (1989) 231–249
Elsevier Sequoia S.A., Lausanne – Printed in The Netherlands
JOM 09875

# Mass spectrometric studies of some bis($\eta^5$-pentamethylcyclopentadienyl)metal derivatives, and related complexes

**F. Geoffrey N. Cloke, Jeremy P. Day, Anthony M. Greenway, Kenneth R. Seddon *, Amer A. Shimran and Anthony C. Swain**

*School of Chemistry and Molecular Sciences, University of Sussex, Falmer, Brighton BN1 9QJ (Great Britain)*

(Received November 10th, 1988)

## Abstract

A series of bis(pentamethylcyclopentadienyl)metal derivatives, and related complexes, including $[Mo(C_5Me_5)_2X_2]$ ($X_2 = H_2$, $Cl_2$, $I_2$ or O), $[W(C_5Me_5)_2X_2]$ (X = H, Cl or $CH_3$), $[W(C_5Me_5)(C_5Me_4CH_2)Cl]$, $[Re(C_5Me_5)_2]$, $[Re(C_5Me_5)(C_5Me_4CH_2)]$, $[Re(C_5Me_5)_2(NO)]$, $[Rh(C_5Me_5)(C_5Me_5H)]$, $[Rh(C_5Me_5)_2][BF_4]$, $[\{Rh(C_5Me_5)X_2\}_2]$ (X = Cl, Br or I), and $[M(C_5Me_5)_2]$ (M = Fe or Ru) have been investigated by mass spectrometry using different ionization techniques, viz. electron impact (EI), chemical ionization (CI) and fast-atom bombardment (FAB). The fragmentation pathways were confirmed by observation of metastable transitions for the spectra obtained by EI. For both FAB and EI spectra, the identities of the molecular ions and major metal-containing fragment ions were confirmed by fitting to computer-simulated isotopic abundance patterns. Intramolecular oxidative addition reactions, to form cyclometallated species via sixteen-electron intermediates, were observed for rhenium, molybdenum and tungsten complexes in the gas phase; these parallel known behaviour in solution. In contrast, the complexes of iron, ruthenium and rhodium, which do not achieve a sixteen-electron configuration, fragment via the loss of methyl groups.

## Introduction

A significant advance in the study of metallocene chemistry was made when the cyclopentadienyl ($C_5H_5$) ligand was replaced by the pentamethylcyclopentadienyl ($C_5Me_5$) ligand. The greater electron-donating nature of the $C_5Me_5$ ligand produces a stronger ligand–metal bond, while its greater bulk stabilizes complexes of lower coordination number. Following its introduction by King [1], its chemistry was

0022-328X/89/$03.50 

expanded by Wolczanski and Bercaw [2] for titanium and zirconium systems, and by Maitlis [3] for the preparation of rhodium and iridium systems.

A large number of bis($\eta^5$-cyclopentadienyl)metal derivatives have been investigated by mass spectrometry (MS) [4–8], but few related studies of bis(pentamethylcyclopentadienyl)metal complexes have appeared in the literature [9–11]. As an extension of our interest in bis(cyclopentadienyl)metal derivatives [8], we have carried out mass spectral analyses on a series of bis($\eta^5$-pentamethylcyclopentadienyl)metal derivatives, and related complexes, including $[Mo(C_5Me_5)_2X_2]$ ($X_2$ = $H_2$ (**1**), $Cl_2$ (**2**), $I_2$ (**3**) or O (**4**)); $[W(C_5Me_5)_2X_2]$ (X = H (**5**), $CH_3$ (**6**) or Cl (**7**)); $[W(C_5Me_5)(C_5Me_4CH_2)Cl]$ (**8**); $[Re(C_5Me_5)_2]$ (**9**); $[Re(C_5Me_5)(C_5Me_4CH_2)]$ (**10**); $[Re(C_5Me_5)_2(NO)]$ (**11**) and $[Rh(C_5Me_5)(C_5Me_5H)]$ (**12**) which are all air-sensitive, and $[Rh(C_5Me_5)_2][BF_4]$ (**13**); $[\{Rh(C_5Me_5)X_2\}_2]$ (X = Cl (**14**), Br (**15**) or I (**16**)) and $[M(C_5Me_5)_2]$ (M = Fe (**17**) or Ru (**18**)).

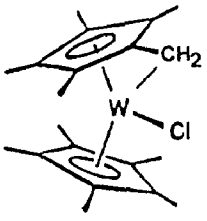


(8)

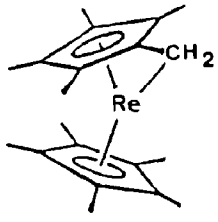


(10)

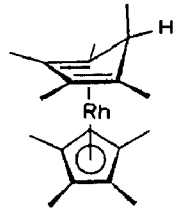


(12)

According to the literature reports on these complexes, only $[\{Rh(C_5Me_5)Cl_2\}_2]$ [12], $[Fe(C_5Me_5)_2]$ [11] and $[Ru(C_5Me_5)_2]$ [13] have been previously investigated by mass spectrometry.

Although some of these complexes are sufficiently volatile to study under electron-impact (EI) and chemical ionization (CI) conditions, the technique of fast-atom bombardment mass spectrometry (FAB-MS) was necessary for complexes with ionic character or low volatility.

## Experimental

Mass spectra were obtained with a Kratos Analytical Ltd. (Manchester, UK) MS80RF double focusing mass spectrometer interfaced to a Kratos DS55M data system.

The EI and CI mass spectra were produced with electron energies of 70 and 150 eV and trap currents of 100 and 500 $\mu$A, respectively; a heatable direct-insertion probe was used as necessary with a source temperature of 250 °C. Resolution (10% valley definition) was approximately 1000 at an accelerating voltage of 4 kV. Ammonia was used as the chemical ionization reagent gas. The air-sensitive samples were stored prior to analysis in glass capillary tubes filled with argon, and were opened and placed in the direct-insertion probe under dinitrogen.

FAB-MS was carried out using a dedicated Kratos ion source fitted with an Ion Tech Ltd. (Teddington, UK) atom gun. The bombarding gas, xenon (Research Grade, BOC Ltd.), was used at an atom-beam energy of 6–8 kV. Samples were dissolved in the matrix liquid, 3-nitrobenzyl alcohol (Fluka Chemical Ltd.), and

coated on a stainless-steel platform. The ion source was operated at room temperature; the resolution was between 1000 and 3000 and the accelerating voltage at 4 kV.

Mass scan speeds were 3 s decade$^{-1}$ for the EI and CI spectra, and 30 s decade$^{-1}$ for FAB mass spectra.

By linking the magnetic field ($B$) and the electrostatic analyzer voltage ($E$) such that a constant $B:E$ ratio was maintained during scans ($B/E$ scans), spectra showing daughter ions derived from decompositions occurring in the first field-free region of the MS80RF mass spectrometer provided confirmation of fragmentation pathways.

The complexes **14–16** [12,14], (**17**) [1] and **18** [13] were prepared by simple variations on the earlier published methods. The complexes **1–12** were prepared by metal atom synthesis, in a manner similar to previously reported methods [15–17]. The salt **13** was prepared from **12** by hydride abstraction with $[CPh_3][BF_4]$ [15].

## Results and discussion

*Rhodium complexes*

According to Booth and coworkers [12], the EI mass spectrum of $[\{Rh(C_5Me_5)Cl_2\}_2]$ (**14**) shows neither the molecular ion nor the $[M - Cl]^+$ fragment ion. The observed base peak of their spectrum was due to the $[C_5Me_4CH_2]^{+\cdot}$ ion, $m/z$ 134; we confirm this report. However, the positive FAB mass spectra of this complex (and its bromide and iodide analogues, **15** and **16**) yield significantly more useful information; the spectrum of **14** shows both a molecular ion and the $[M - Cl]^+$ fragment ion (see Fig. 1), while those of **15** and **16** give a $[M - X]^+$ ion (X = Br or I) as their highest mass ion (Table 1). Recently [18], similar behaviour was observed in the FAB mass spectra of some platinum and palladium coordination complexes $[M(LL)X_2]$ (LL = bidentate phosphine ligands), where the base peak of most of those complexes was due to the $[M - X]^+$ fragment ion, with only a weak molecular ion being observed (if present at all).

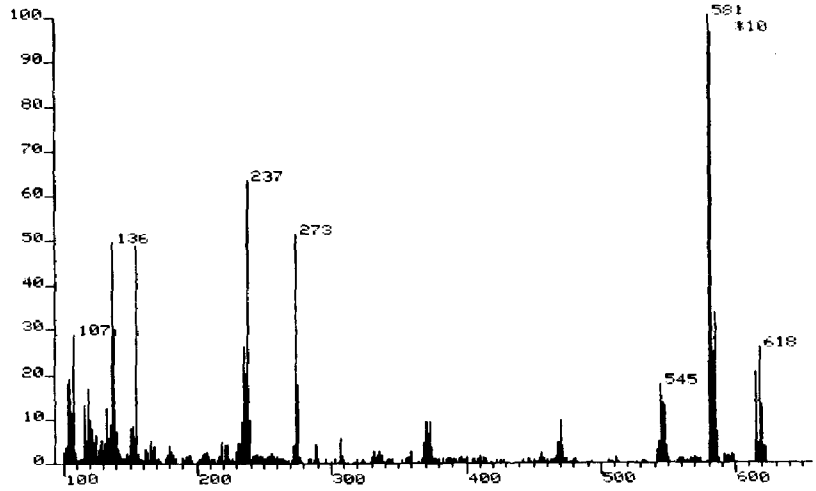


Fig. 1. The positive FAB mass spectrum of $[\{Rh(C_5Me_5)Cl_2\}_2]$ (**14**).

Table 1

Major metal-containing fragment ions in the mass spectra of the rhodium complexes **12**, **14**, **15** and **16**

| Fragment ion | $m/z$ [a] and % relative abundances [b] | | | |
|---|---|---|---|---|
| | $[\{Rh(C_5Me_5)X_2\}_2]$ [c] | | | $[Rh(C_5Me_5)(C_5Me_5H)]$ [d] |
| | X = Cl | X = Br | X = I | |
| $M^{+\cdot}$ | 616(3) | | | 374(11) |
| $[Rh(C_5Me_5)_2]^+$ | | | | 373(5) |
| $[Rh(C_5Me_5)(C_5Me_4H)]^+$ | | | | 359(100) |
| $[Rh(C_5Me_5)(C_5Me_3H)]^{+\cdot}$ | | | | 344(2) |
| $[M-X]^+$ | 581(100) | 713(45) | 857(90) | |
| $[M-2X]^{+\cdot}$ | | | 730(20) | |
| $[M-X\text{-}HX]^+$ | 545(20) | 633(10) | 729(18) | |
| $[M-2X-C_5Me_5]^+$ | | | 595(4) | |
| $[M-4HX-2H]^{+\cdot}$ | 470(10) | 470(2) | | |
| $[M-3HX-C_5Me_5]^{+\cdot}$ | 370(10) | | 465(4) | |
| $[Rh(C_5Me_5)X_2]^{+\cdot}$ | 308(5) | | | |
| $[M-X_2-HX-C_5Me_5]^+$ | | 419(7) | | |
| $[Rh(C_5Me_5)X]^+$ | 273(53) | 317(28) | 365(43) | |
| $[Rh(C_5Me_5H)]^+$ | | | | 239(1.5) |
| $[Rh(C_5Me_5)]^{+\cdot}$ | 238(10) | 238(8) | 238(2) | |
| $[Rh(C_5Me_4CH_2)]^+$ | 237(65) | 237(37) | 237(15) | |
| $[Rh(C_5Me_4H)]^+$ | | | | 224(10) |
| $[Rh(C_5Me_3H)]^{+\cdot}$ | | | | 209(2) |

[a] Nominal mass, using the lowest mass isotopes of each element. [b] Relative intensities are normalized to the most intense metal-containing fragment ion, and given in parentheses. [c] Positive FAB spectra. [d] 70 eV EI spectrum.

A fragmentation pathway for complexes **14–16** is proposed, using **14** as an example (see Fig. 2). Good agreement between the experimental and computer simulated isotopic patterns for $[\{Rh(C_5Me_5)X_2\}_2]$ (X = Cl or Br), in the molecular ion and/or $[M-X]^+$ fragment ion regions, was obtained (Fig. 3).

The EI mass spectrum of $[Rh(C_5Me_5)(C_5Me_5H)]$ (**12**) shows a molecular ion of low intensity, $m/z$ 374. This ion loses either a hydrogen radical to form a $[Rh(C_5Me_5)_2]^+$ fragment ion, $m/z$ 373, or a methyl radical giving a $[Rh(C_5Me_5)(C_5Me_4H)]^+$ ion, $m/z$ 359, as the base peak of the spectrum (Fig. 4); both losses were confirmed by metastable transitions.

The ionic compound $[Rh(C_5Me_5)_2][BF_4]$ (**13**) was investigated by both positive and negative FAB-MS. The positive FAB spectrum gives an ion at $m/z$ 373, due to the cation $[Rh(C_5Me_5)_2]^+$, which is also the base peak. A weak ion at $m/z$ 833 (Fig. 5(a)) due to a 2:1 cation-anion aggregate, viz. $[\{Rh(C_5Me_5)_2\}_2\{BF_4\}]^+$, is also observed; such aggregates have been observed for other metal complexes using FAB-MS [19]. No ion was observed corresponding to $[Rh(C_5Me_5)_2][BF_4]$. Similarly, the negative FAB spectrum gives a weak ion at $m/z$ 547 which is due to the 1:2 cation-anion aggregate $[\{Rh(C_5Me_5)_2\}\{BF_4\}_2]^-$ and an ion at $m/z$ 87, $[BF_4]^-$, as the base peak of the spectrum (Fig. 5(b)).

The positive FAB mass spectra of **13**, **14**, **15** and **16** all show an ion at $m/z$ 238 due to the $[Rh(C_5Me_5)]^{+\cdot}$ ion, which then exhibits successive loss of hydrogen radicals.

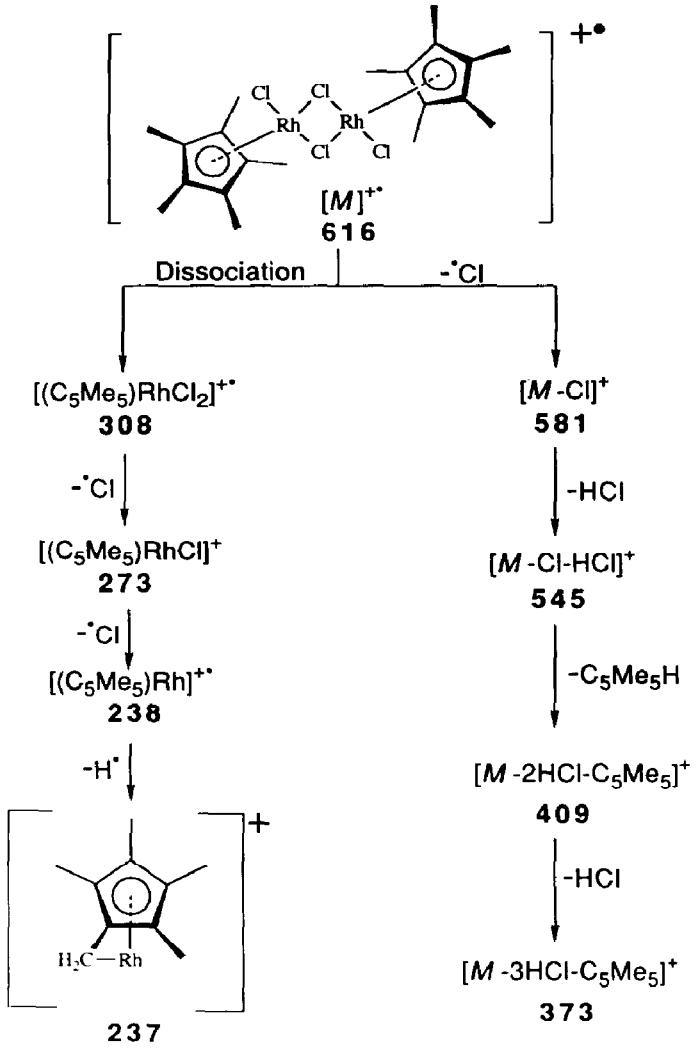


Fig. 2. The proposed key fragmentation pathways for $[\{Rh(C_5Me_5)Cl_2\}_2]$ (**14**).

*Iron and ruthenium complexes*

While a detailed mass spectrometric investigation has been reported for the $[Fe(C_5Me_5)_2]$ (**17**) [11], there is no detailed report for its ruthenium analogue (**18**). During this work, the EI mass spectra of **17** and **18** were obtained; both show the molecular ion as the base peak of their spectra (Fig. 6), with fragment ions of relatively low intensity (owing to the high stability of these complexes). The doubly charged molecular ions at $m/z$ 163 and 186 in the spectra of **17** and **18**, respectively, are further evidence of the high stability of these complexes. Good agreement between the experimental and the computer simulation of the isotopic pattern in the molecular ion region of **18** was obtained. Table 2 shows the major metal-containing fragment ions of these two complexes. The fragmentation pathways, as confirmed by metastable transitions, are similar for **17** and **18** and correspond to that reported earlier [11].

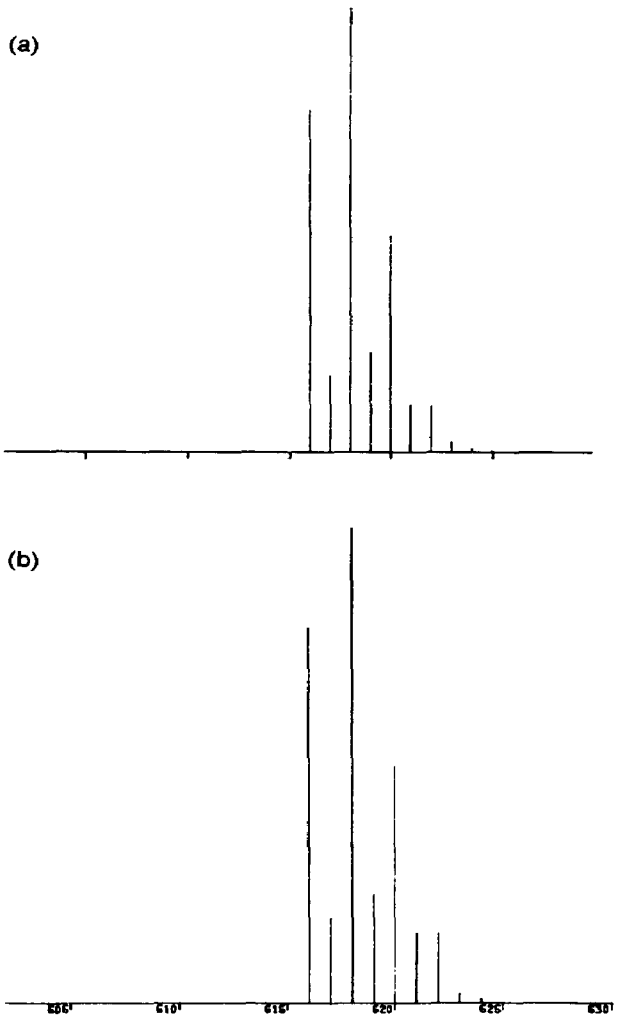


Fig. 3. (a) A computer simulation of, and (b) the experimental isotopic pattern for, the molecular ion of $[\{Rh(C_5Me_5)Cl_2\}_2]$ (**14**).

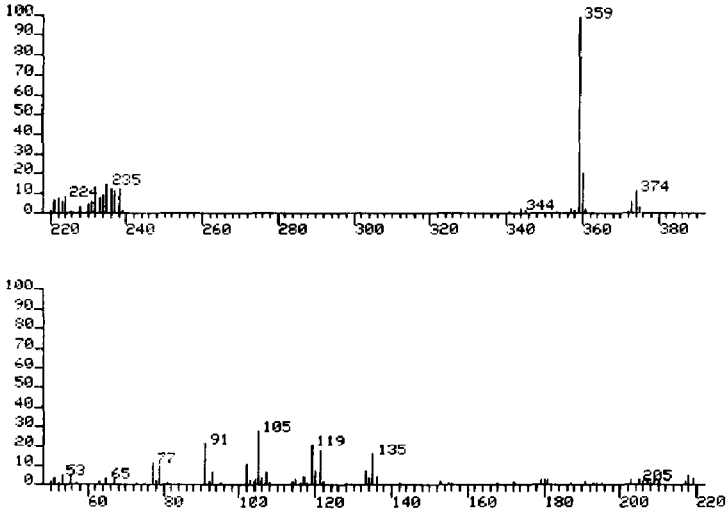


Fig. 4. The EI (70 eV) mass spectrum of $[Rh(C_5Me_5)(C_5Me_5H)]$ (**12**).

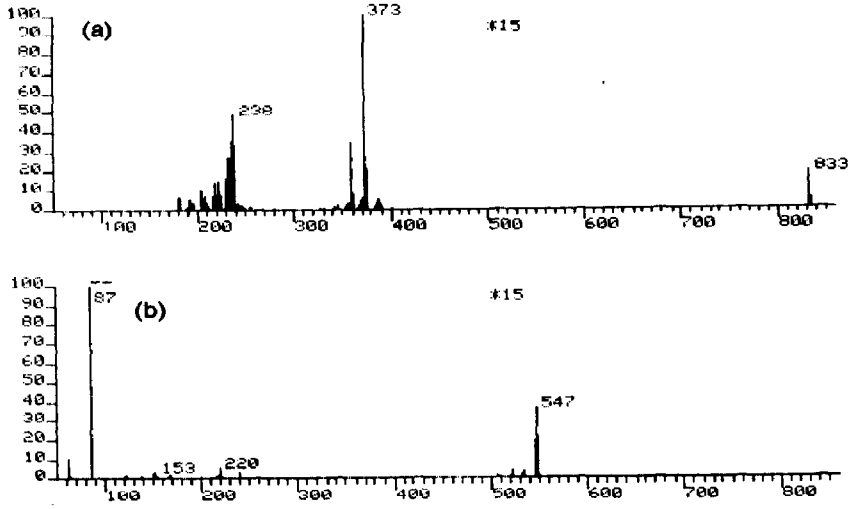


Fig. 5. (a) The positive and (b) negative FAB mass spectra of $[Rh(C_5Me_5)_2][BF_4]$ (13).

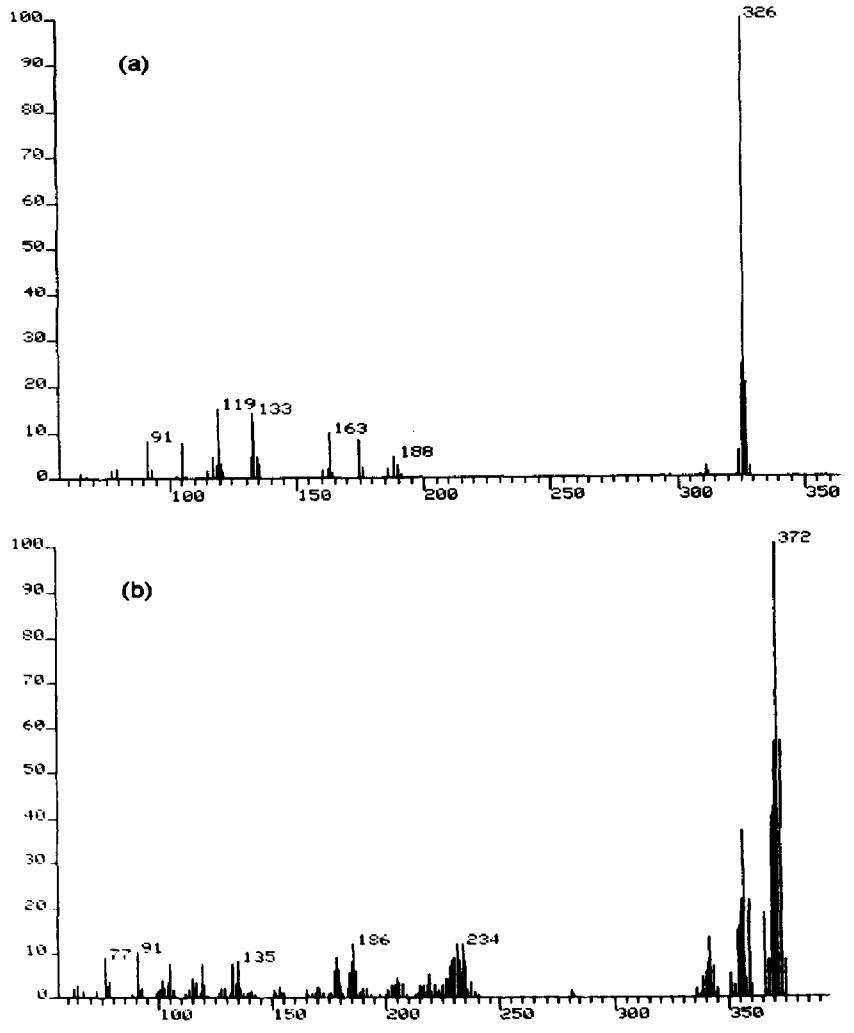


Fig. 6. The EI (70 eV) mass spectra of (a) $[Fe(C_5Me_5)_2]$ (17), and (b) $[Ru(C_5Me_5)_2]$ (18).

The CI mass spectrum of $[Ru(C_5Me_5)_2]$, using ammonia as reagent gas, gives an intense protonated molecular ion, $[M + H]^+$, at $m/z$ 373.

*Rhenium complexes*

The EI mass spectra of $[Re(C_5Me_5)_2]$ (**9**), $[\overline{Re(C_5Me_5)(C_5Me_4CH_2)}]$ (**10**) and $[Re(C_5Me_5)_2(NO)]$ (**11**), which have been investigated by mass spectrometry for the first time here, were obtained. Rhenium exists as two isotopes, one of mass 184.9530 (37.07%) and the other of 186.9560 (62.98%). The presence of these isotopes gives rise to a spread or 'envelope' of ions for a given nominal mass; rhenium-containing ion species can easily be recognized by comparing the experimental distribution pattern of the envelope with that of the computer simulation for the theoretical distribution. High resolution was employed for the accurate mass measurement of

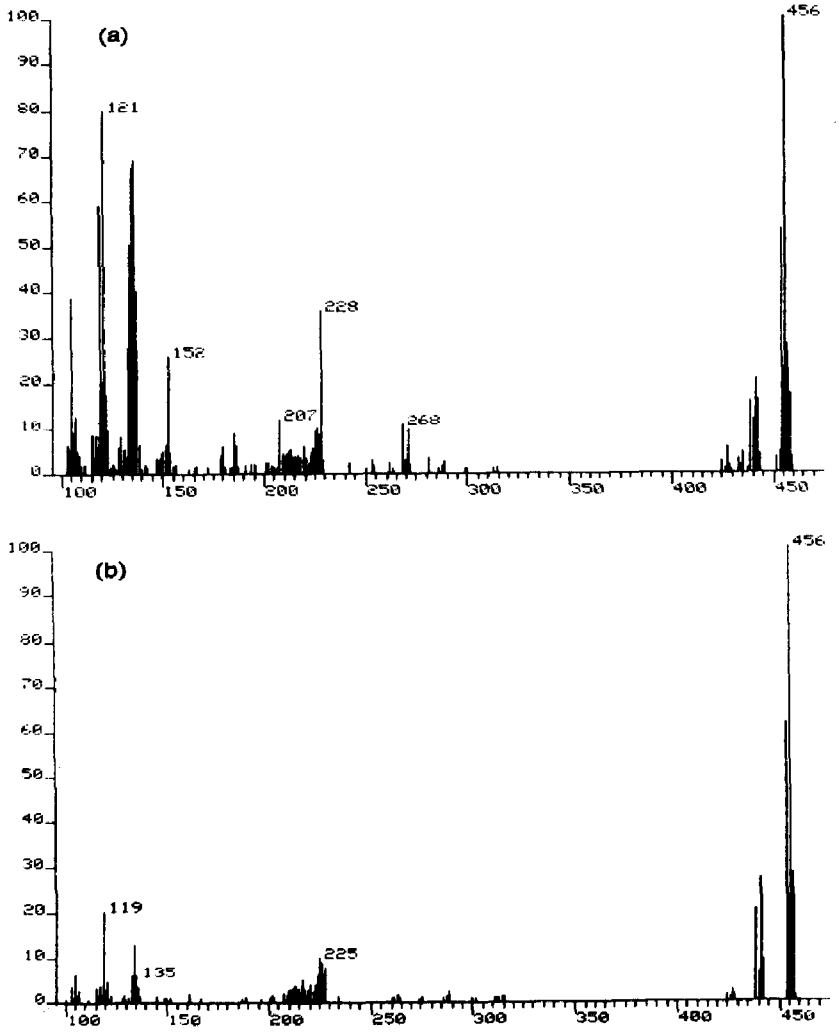


Fig. 7. The EI (70 eV) mass spectra of (a) $[Re(C_5Me_5)_2]$ (**9**), (b) $[\overline{Re(C_5Me_5)(C_5Me_4CH_2)}]$ (**10**), (c) $[Re(C_5Me_5)_2(NO)]$ (**11**), and (d) the CI (reagent gas, $NH_3$) mass spectrum of **11**.

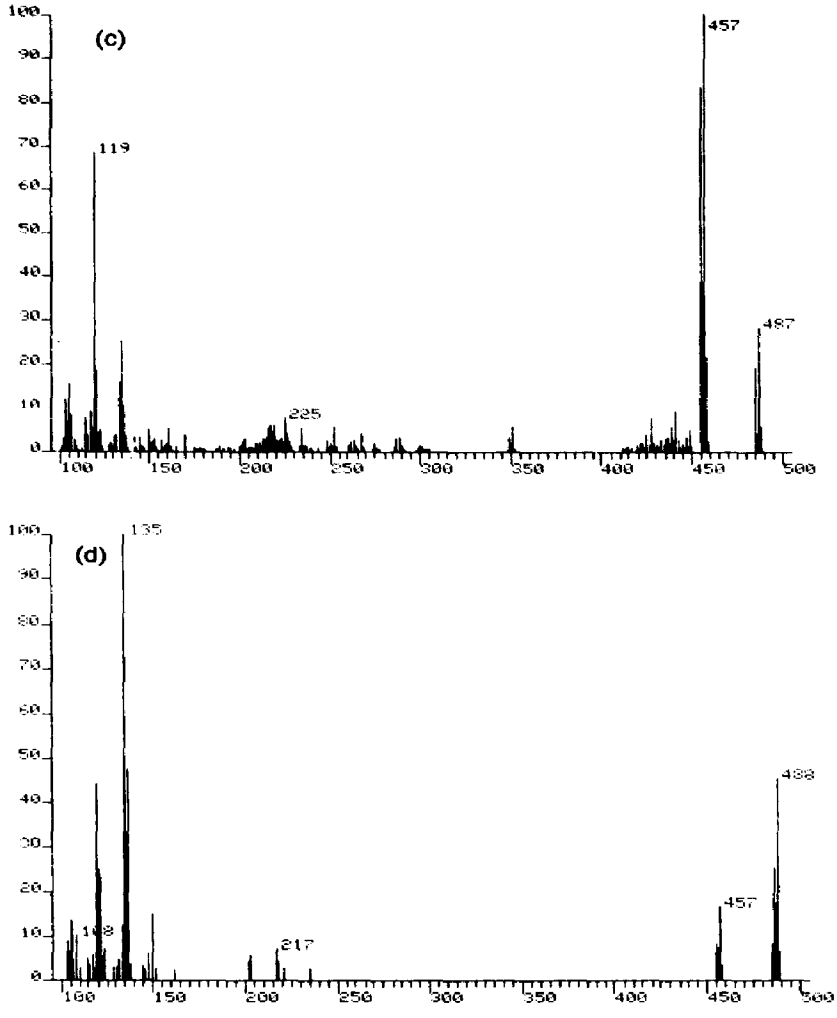


Fig. 7 (continued).

Table 2

Major metal-containing fragment ions in the mass spectra of the iron and ruthenium complexes **17** and **18**

| Fragment ion | *m/z* [a] and % relative abundances [b] | | |
|---|---|---|---|
| | $[Fe(C_5Me_5)_2]$ | $[Ru(C_5Me_5)_2]$ | |
| | EI | EI | CI |
| $M^{+\cdot}$ | 326(100) | 372(100) | 373(100) |
| $[M-CH_3]^+$ | 311(2.5) | 357(40) | 357(5) |
| $[M-2CH_3]^{+\cdot}$ | 296(1) | 342(15) | |
| $[M-C_5Me_5]^+$ | 191(0.6) | 237(5) [c] | |
| $[M-C_5Me_5-H]^{+\cdot}$ | 190(0.3) | 236(4) [c] | |
| $[M-C_5Me_5-2H]^+$ | 189(3) | 235(9) [c] | |
| $[M-C_5Me_5-3H]^{+\cdot}$ | 188(5) | 234(13) [c] | |
| $[M-C_5Me_5-CH_3-2H]^+$ | 174(8) | 219(6) | |
| $[M-C_5Me_5-2CH_3-H]^{+\cdot}$ | 160(2) | 206(2) | |
| $M^{2+}$ | 163(10) | 186(12) | |

[a] Nominal mass, using the lowest mass isotopes of each element. [b] Relative intensities are normalized to the most intense metal-containing fragment ion, and given in parentheses. [c] Overlap between the isotopic distributions of neighbouring ions means that these relative intensities are only approximate.

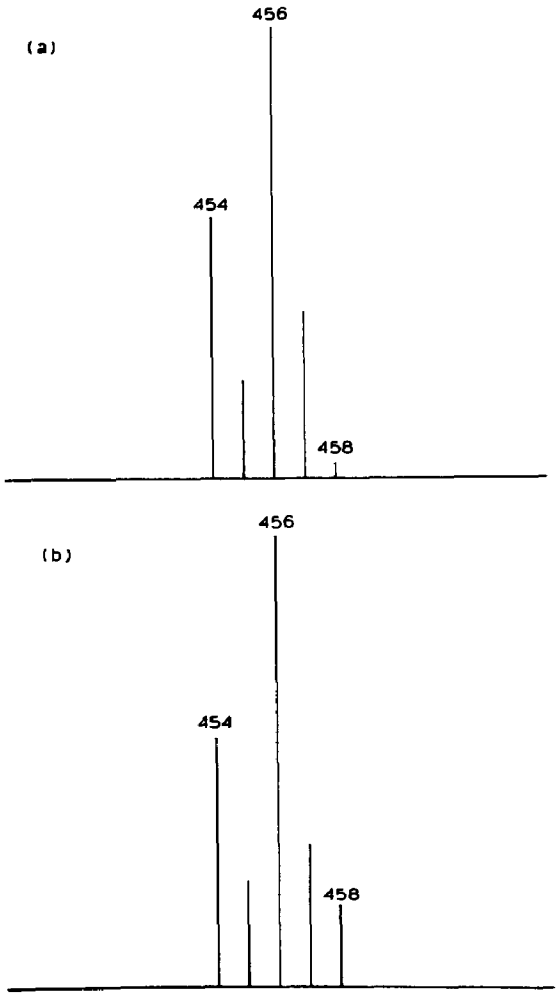


Fig. 8. (a) A computer simulation of, and (b) the experimental isotopic pattern for, $[Re(C_5Me_5)_2]$ (**9**), in the region of the overlapping ions $M^{+\cdot}$ (**19**), and $[M-1]^+$ (**20**).

Table 3

Major metal-containing fragment ions in the EI mass spectra of the rhenium complexes **9**, **10** and **11**

| Fragment ion | $m/z$ [a] and % relative abundances [b] | | |
|---|---|---|---|
| | $[Re(C_5Me_5)_2(NO)]$ | $[Re(C_5Me_5)_2]$ | $[Re(C_5Me_5)(C_5Me_4CH_2)]$ |
| $[Re(C_5Me_5)_2(NO)]^{+\cdot}$ | 487(32); $M^{+\cdot}$ | | |
| $[Re(C_5Me_5)_2]^{+\cdot}$ | 457(100) [c] | 457(30) [c]; $M^{+\cdot}$ | |
| $[Re(C_5Me_5)(C_5Me_4CH_2)]^+$ | 456(43) [c] | 456(100) [c] | 456(100); $M^{+\cdot}$ |
| $[Re(C_5Me_5)(C_5Me_4)]^+$ | 442(2) [c] | 442(18) [c] | |
| $[Re(C_5Me_5)(C_5Me_3CH_2)]^{+\cdot}$ | 441(10) [c] | 441(21) [c] | 441(30) |
| $[Re(C_5Me_5)(C_5Me_3)]^{+\cdot}$ | 427(7) [c] | 427(7) [c] | 427(3) [c] |
| $[Re(C_5Me_5)(C_5Me_2CH_2)]^+$ | 426(2) [c] | 426(1) [c] | 426(1) [c] |
| $[Re(C_5Me_4CH_2)(NO)]^{+\cdot}$ | 351(8) | | |

[a] Nominal mass, using the lowest mass isotopes of each element. [b] Relative intensities are normalized to the most intense metal-containing fragment ion, and given in parentheses. [c] Overlap between the isotopic distributions of neighbouring ions means that these relative intensities are only approximate.

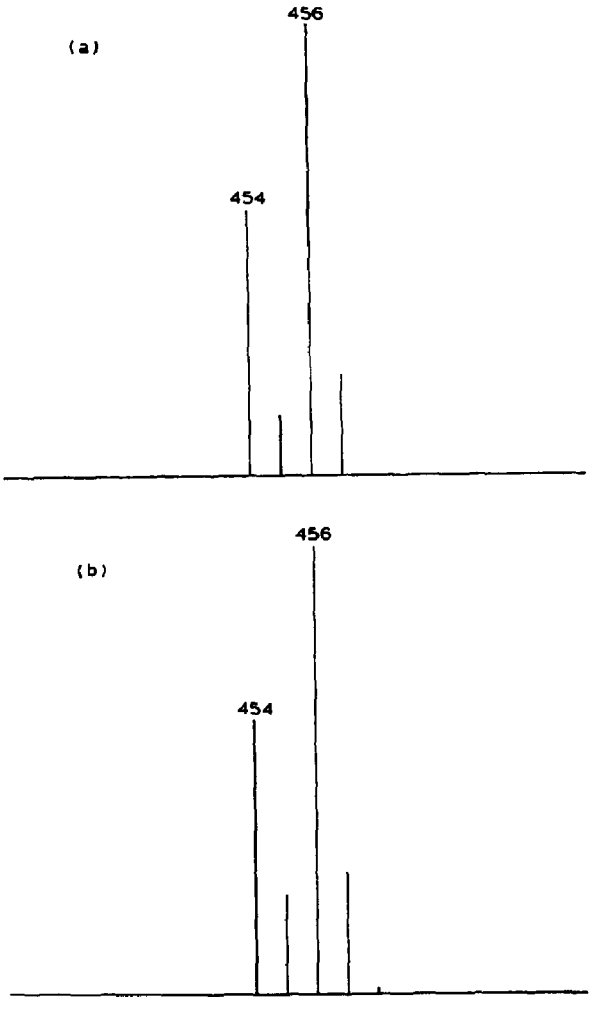


Fig. 9. (a) A computer simulation of, and (b) the experimental isotopic pattern for, the molecular ion (**20**) of $[\dot{R}e(C_5Me_5)(C_5Me_4\dot{C}H_2)]$ (**10**).

the molecular ion region of these compounds, and the main fragmentation processes confirmed by metastable transition studies.

The EI mass spectrum of $[Re(C_5Me_5)_2]$ (**9**) (Fig. 7(a)) shows an ion at $m/z$ 456 (based on $^{187}Re$), confirmed by a metastable transition to be formed by loss of a hydrogen radical from the molecular ion **19**, and believed to have a structure as shown in **20**. Since $[M-1]^+$ is more intense than $[M]^{+\cdot}$, it was assumed that structure **20** was more stable than structure **19**; the overlap of the 'envelope' of ions for $[M]^{+\cdot}$ and $[M-1]^+$ (Fig. 8(a)) was computer simulated (Fig. 8(b)) and leads to an estimate of the relative amounts of **19** and **20** being 14 and 86% respectively. The assignment of the $[M-1]^+$ ion to **20** was supported by obtaining the EI mass spectrum of $[\dot{R}e(C_5Me_5)(C_5Me_4\dot{C}H_2)]$ (**10**), (Fig. 7(b) and Table 3); the molecular ion, which is also the base peak, here must have structure **20** and shows an excellent agreement between the actual and computer simulated ion distribution (see Fig. 9).

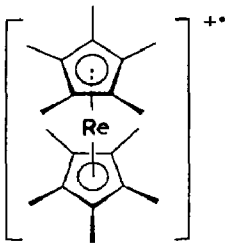


(19)

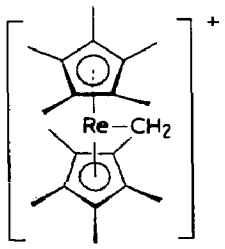


(20)

The EI mass spectrum of $[Re(C_5Me_5)_2(NO)]$ (**11**) (Fig. 7(c) and Table 3) gives a molecular ion, *m/z* 487, of approximately 30% relative intensity and an ion at *m/z* 457 as the base peak of the spectrum. This ion was confirmed by metastable transition to be produced directly from the molecular ion as a result of losing NO, to give an ion of structure (**19**) which then, as expected, loses a hydrogen radical to give an ion of structure **20** at *m/z* 456. The CI mass spectrum of $[Re(C_5Me_5)_2(NO)]$ gives a protonated molecular ion $[M + H]^+$ at *m/z* 488, Fig. 7(d), more intense than $[M]^{+\cdot}$, in its EI spectrum, and a weak fragment ion **19**, which again overlaps with **20**, as in the EI spectrum. In addition, ions due to cracking of the $C_5Me_5^-$ ligand were observed.

*Molybdenum and tungsten complexes*

The EI mass spectrometric data for $[M(C_5Me_5)_2X_2]$ **1–7** (Tables 4 and 5), represent the first detailed investigation of these novel complexes, which all exhibit molecular ions. Moreover, they behave similarly in the gas phase in that, after the loss of $X_2$ (M = Mo; $X_2 = H_2$, $Cl_2$, $I_2$ or O; M = W, X = H, Cl or $CH_3$), the resulting ion $[M(C_5Me_5)_2]^+$ (**21**) (M = Mo or W), is subjected to immediate loss of $H_2$ from the methyl groups to form the ion $[M(C_5Me_5)\{C_5Me_3(CH_2)_2\}]^+$ (**22**). A

Table 4

Major metal-containing fragment ions in the EI mass spectra of the molybdenum complexes **1**, **2**, **3** and **4**

| Fragment ion | *m/z* [a] and % relative abundances [b] | | | |
|---|---|---|---|---|
| | $[Mo(C_5Me_5)_2X_2]$ | | | |
| | $X_2 = H_2$ | $X_2 = Cl_2$ | $X_2 = I_2$ | $X_2 = O$ |
| $M^{+\cdot}$ | 370(20) [c] | 438(37) | 622(40) | 384(70) |
| $[M - CH_3]^+$ | | | 607(3) | |
| $[M - X]^+$ | 369(25) [c] | 403(28) | 495(100) | |
| $[M - 2X]^{+\cdot}$ | 368(17) [c] | 368(17) [c] | 368(47) [c] | 368(56) [c] |
| $[M - 2X\text{-}H]^+$ | 367(60) [c] | 367(15) [c] | 367(67) [c] | |
| $[M - 2HX]^{+\cdot}$ | 366(100) [c] | 366(16) [c] | 366(70) [c] | 366(100) [c] |
| $[M - C_5Me_5H]^{+\cdot}$ | | 302(20) | 486(4) | 248(8) [c] |
| $[M - C_5Me_5H\text{-}2H]^{+\cdot}$ | | | | 246(12) [c] |
| $[M - 2X - CH_3]^+$ | 353(12) [c] | | | |
| $[M - 2HX - CH_3]^+$ | 351(24) [c] | | | |
| $[M - C_5Me_5H - HX]^{+\cdot}$ | | 266(55) | 358(49) | |
| $[Mo(C_3Me_3H_2)]^+$ | 181(20) | 181(5) | 181(22) | 181(2) |

[a] Nominal mass, using the lowest mass isotopes of each element. [b] Relative intensities are normalized to the most intense metal-containing fragment ion, and given in parentheses. [c] Overlap between the isotopic distributions of neighbouring ions means that these relative intensities are only approximate.

Table 5

Major metal-containing fragment ions in the EI mass spectra of the tungsten complexes **5**, **6**, **7** and **8**

| Fragment ion | $m/z$ [a] and % relative abundances [b] | | | |
|---|---|---|---|---|
| | $[W(C_5Me_5)_2X_2]$ | | | $[W(C_5Me_5)(C_5Me_4CH_2)Cl]$ |
| | X = H | X = $CH_3$ | X = Cl | |
| $M^{+\cdot}$ | 456(75) [c] | 484(5) | 524(46) | 488(100) |
| $[M-X]^+$ | 455(55) [c] | | 489(79) | |
| $[M-CH_3]^+$ | | | | 473(35) |
| $[M-HX]^{+\cdot}$ | 454(100) [c] | 468(6) | | 452(56) |
| $[M-2X]^{+\cdot}$ | 454(100) [c] | 454(29) [c] | 454(20) [c] | |
| $[M-2HX]^{+\cdot}$ | 452(80) [c] | 452(27) [c] | 452(11) [c] | |
| $[M-2X-CH_3]^+$ | 439(7) [c] | | | |
| $[M-2X-CH_3-H]^{+\cdot}$ | | 438(5) | | |
| $[M-2X-CH_3-2H]^+$ | 437(10) [c] | | | |
| $[M-C_5Me_5H]^{+\cdot}$ | | | 390(30) | 352(60) |
| $[M-C_5Me_5H-CH_3]^+$ | | | | 337(8) |
| $[M-C_5Me_5H-XH]^{+\cdot}$ | | | 352(15) | |
| $[M-2X-C_8H_7]^{+\cdot}$ | | 351(22) | | |

[a] Nominal mass, using the lowest mass isotopes of each element. [b] Relative intensities are normalized to the most intense metal-containing fragment ion, and given in parentheses. [c] Overlap between the isotopic distributions of neighbouring ions means that these relative intensities are only approximate.

species of such structure with tungsten has been reported [17] as dark orange crystals, prepared in pentane by the photolysis of $[W(C_5Me_5)_2H_2]$ (**5**), and it is of some interest that these complexes behave in a similar manner under the effect of photolysis and electron bombardment. The envelopes for **21** and **22**, therefore, overlap producing an overall envelope of ions extending over a wide range of masses, Fig. 10(b). The intensity of the individual ions within this envelope depends on the percentages of the ionic species present, and the experimental data can only be fitted, Fig. 10(a), if the presence of a small amount of $[\overline{M(C_5Me_5)(C_5Me_4CH_2)}]^+$ is also assumed. These observations indicate that the ion **21** is must less stable than ion **22**. Of course, in the case of $[M(C_5Me_5)_2H_2]$ (M = Mo or W), the distribution pattern is further complicated as it comprises five ionic species, viz. $[\underline{M(C_5Me_5)_2H_2}]^{+\cdot}$, $[M(C_5Me_5)_2H]^+$, $[M(C_5Me_5)_2]^{+\cdot}$, $[\overline{M(C_5Me_5)(C_5Me_4CH_2)}]^+$ and $[\overline{M(C_5Me_5)\{C_5Me_3(CH_2)_2\}}]^{+\cdot}$, extending over $m/z$ 360–374 in the case of molybdenum (*vide infra*), and over $m/z$ 450–459 in the case of tungsten.

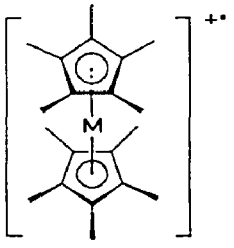


(21)

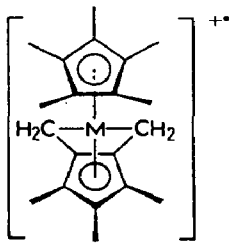


(22)

The EI spectra of complexes **2**, **3**, **6**, **7** and **8** gave, in addition to their molecular ions, fragment ions such as $[M-X]^+$ (X = Cl, I or $CH_3$) and $[M-C_5Me_5H]^{+\cdot}$.

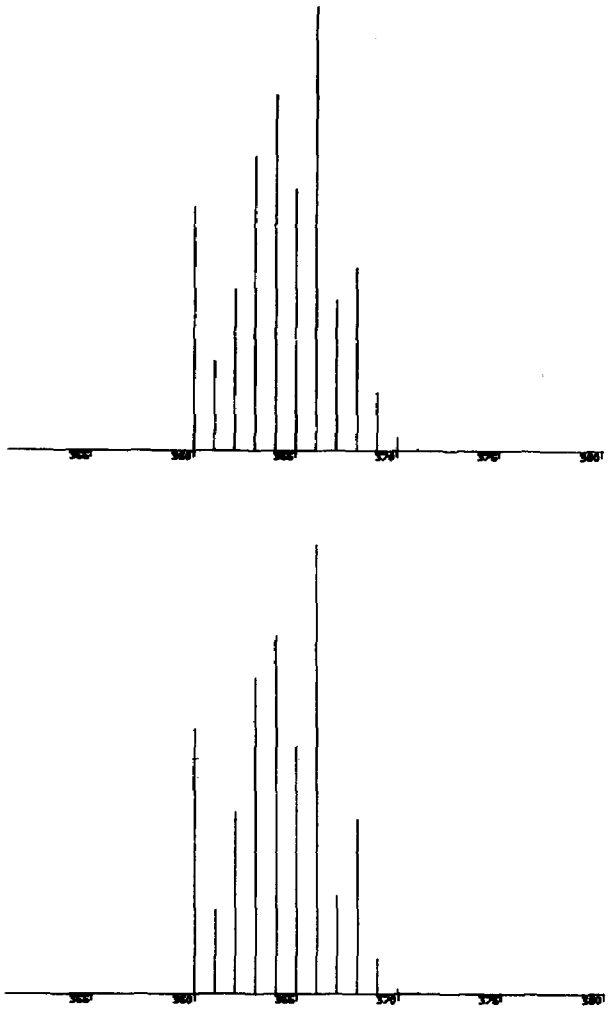

Fig. 10. (a) A computer simulation of, and (b) the experimental isotopic pattern for the ions $[Mo(C_5Me_5)_2]^+$ (**21**), $[\overline{Mo(C_5Me_5)(C_5Me_4CH_2)}]^+$, and $[\overline{Mo(C_5Me_5)\{C_5Me_3(CH_2)_2\}}]^+$ (**22**).

Figure 11 shows the spectra of **2** and **7**. The computer simulations of the isotopic distribution for the ions $[Mo(C_5Me_5)_2Cl_2]^{+\cdot}$, $[Mo(C_5Me_5)_2Cl]^+$, $[\overline{Mo(C_5Me_4CH_2)}Cl_2]^{+\cdot}$, $[Mo(C_5Me_5)I_2]^+$, $[MoO(C_5Me_5)_2]^+$, $[W(C_5Me_5)_2Cl_2]^{+\cdot}$ and $[W(C_5Me_5)_2(CH_3)_2]^{+\cdot}$, show good agreement with the experimental patterns for these ions.

The fragmentation pathways, as confirmed by metastable transitions, of **2** and **8** are shown in Fig. 12.

*The formation of cyclometallated ions in the gas phase*

The formation of the ions **20** and **22** in the mass spectrometer (in the gas phase) correspond to intramolecular oxidative addition reactions, which parallel known chemical reactions in solution. For the rhenium system, these are summarized in Scheme 1. The reaction, **9** → **23**, can also be induced by oxidation with silver(I) tetrafluoroborate [16]. For the hydrido-molybdenum (or -tungsten) system, viz. **1** or **5**), in addition to the route depicted in Fig. 12(a), there must exist a mechanism not

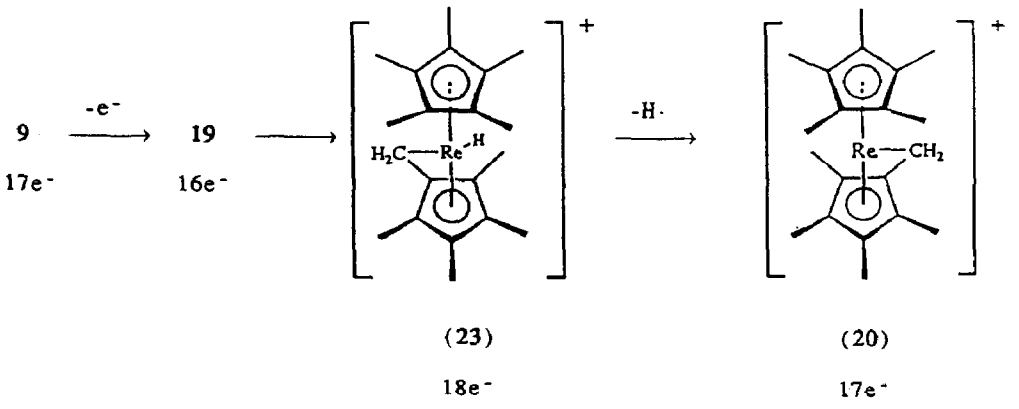


Scheme 1. The gas phase conversion of **9** into **20**.

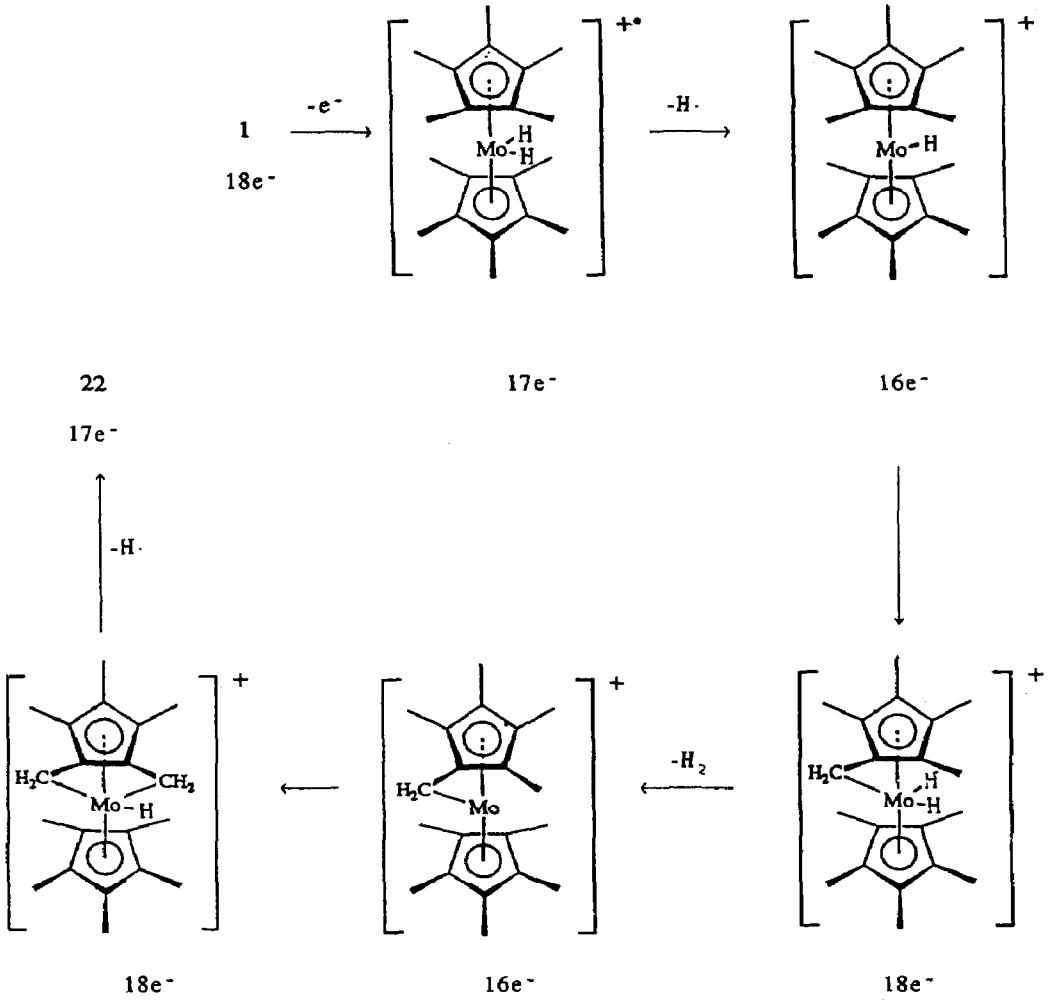


Scheme 2. The gas phase conversion of **1** into **22**.

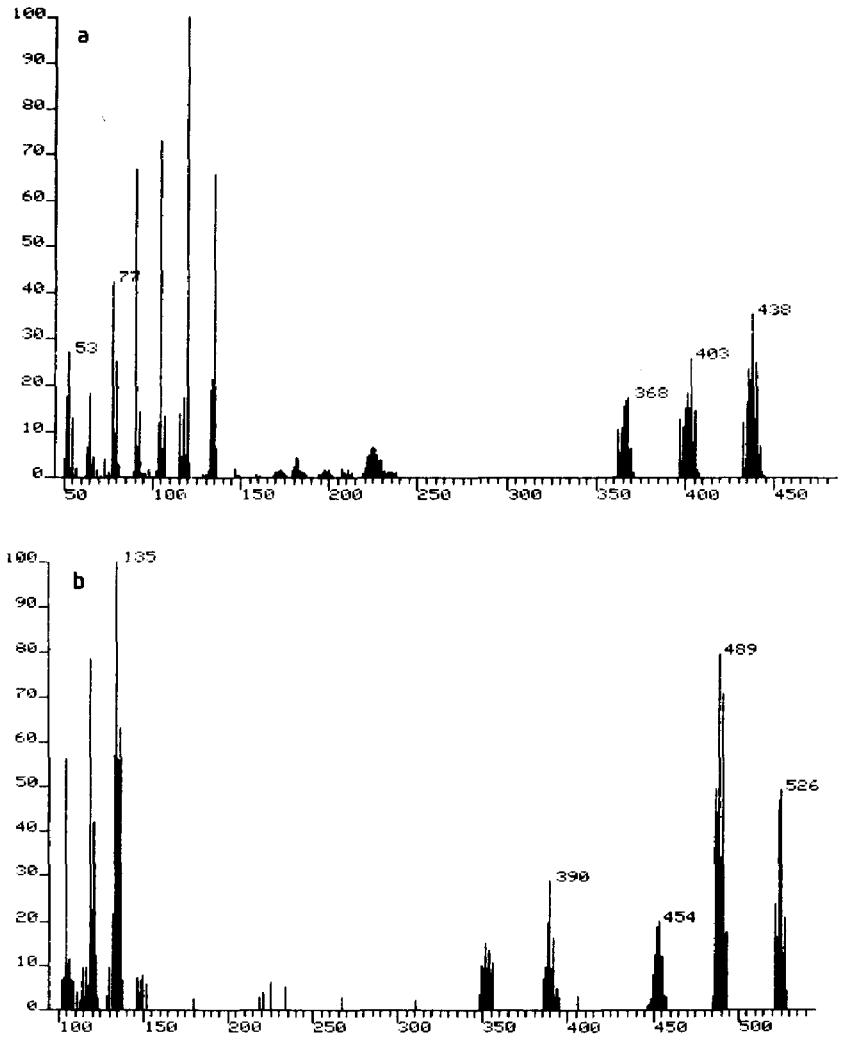


Fig. 11. The EI (70 eV) mass spectra of (a) $[Mo(C_5Me_5)_2Cl_2]$ (**2**), and (b) $[W(C_5Me_5)_2Cl_2]$ (**7**).

involving consecutive stepwise loss of hydrogen radicals, and this is summarized in Scheme 2.

Thus, as could have been expected for rhenium, molybdenum and tungsten, the key oxidative addition steps occurring in the gas-phase (as in solution) are for a sixteen-electron intermediate being converted into an eighteen-electron intermediate. The difference between the gas-phase and solution chemistry is that the gas-phase reactions are all for cations (and hence the final stable species is seventeen-electron, not eighteen-electron), whilst solution chemistry involves neutral molecules. In contrast, the complexes of iron, ruthenium and rhodium, which do not achieve a sixteen-electron configuration, fragment via the loss of methyl groups.

*Fragmentation of the pentamethylcyclopentadienyl ring*

All the above complexes, **1–18**, show fragment ions due to the fragmentation of the pentamethylcyclopentadienyl ligand, $C_5Me_5^-$, which parallel those found for the

parent molecule, $C_5Me_5H$ [20]. Where more than one methyl group has been lost from a fragment ion, we have ascribed this to loss from a single ring; it is equally probable (and we have no evidence for either proposition) that loss occurs from the second ring or, indeed, that both processes occur simultaneously.

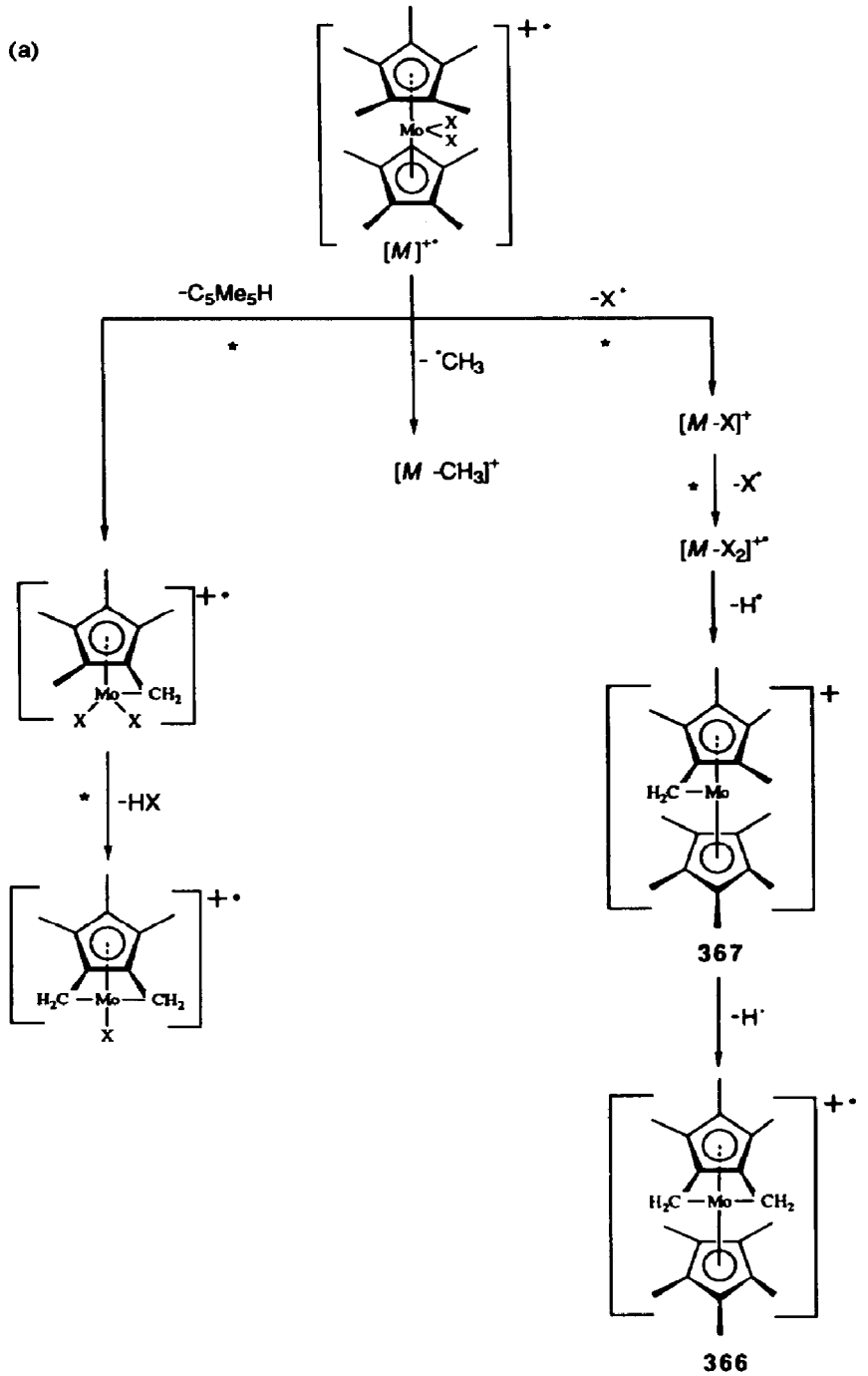


Fig. 12. The key fragmentation pathways for (a) $[Mo(C_5Me_5)_2Cl_2]$ (**2**), and (b) $[W(C_5Me_5)(C_5Me_4CH_2)Cl]$ (**8**); the asterisk denotes those pathways which were confirmed by metastable peaks.

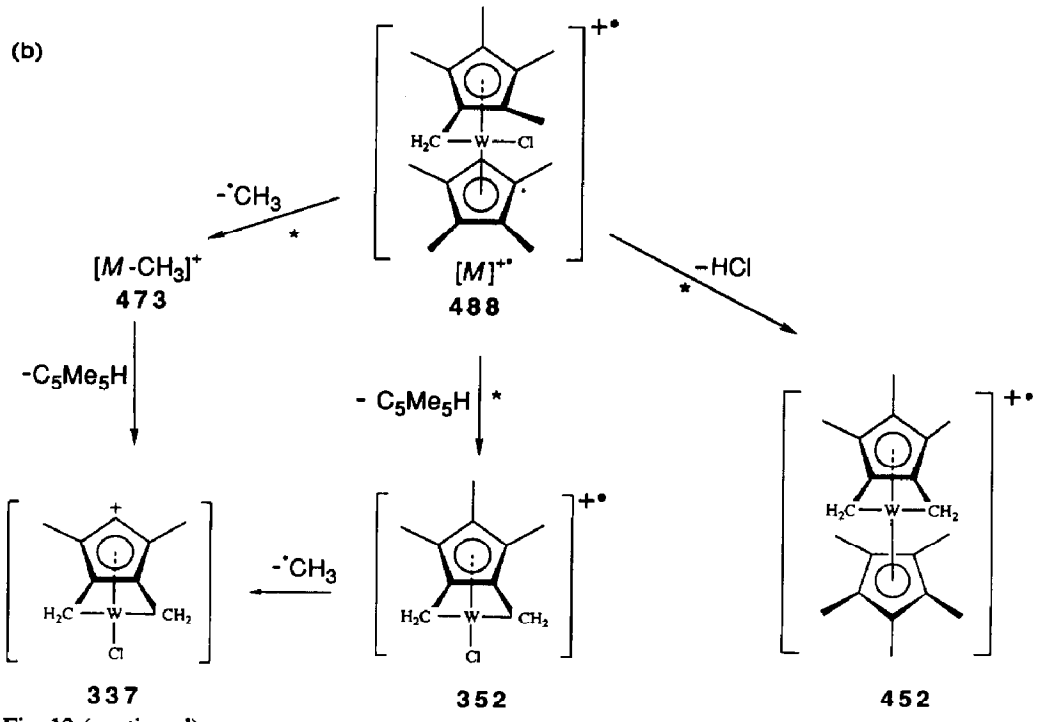


Fig. 12 (continued).

## Conclusions

Apart from establishing its utility for the identification of both molecular and ionic pentamethylcyclopentadienyl complexes, we have shown that mass spectrometry can also give some insight into the possible solution behaviour of these complexes. The existence of a stable cyclometallated ion in the gas phase indicates that such behaviour may also be found in solution.

## Acknowledgements

We are indebted to the S.E.R.C. for two studentships (J.P.D. and A.C.S.), and to the Iraqi government for the award of a research scholarship (A.A.S.).

## References

1 R.B. King and M.B. Bisnette, J. Organomet. Chem., 8 (1967) 287.
2 P.T. Wolczanski and J.E. Bercaw, Acc. Chem. Res., 13 (1980) 121.
3 P.M. Maitlis, Acc. Chem. Res., 11 (1978) 301.
4 D.F. Hunt, J.W. Russell and R.L. Torian, J. Organomet. Chem., 43 (1972) 175.
5 R. Davis and D.J. O'Reardon, J. Indian Chem. Soc., 59 (1982) 1270.
6 G. Innorta, F. Scagnolari, A. Modelli, S. Torroni, A. Foffani and S. Sorriso, J. Organomet. Chem., 241 (1983) 375.
7 G.M. Begun and R.N. Compton, J. Chem. Phys., 58 (1973) 2271.
8 A.M. Al-Saeed, M.C. Grossel, J.P. Knychala, E.A. Seddon, K.R. Seddon, A.A. Shimran and S. Tompkins, J. Organomet. Chem., 347 (1988) C25.

9 J.E. Bercaw, R.H. Marvich, L.G. Bell and H.H. Brintzinger, J. Am. Chem. Soc., 94 (1972) 1219.
10 J.L. Robbins, N.M. Edelstein, S.R. Copper and J.C. Smart, J. Am. Chem. Soc., 101 (1979) 3853.
11 E.I. Mysove, I.R. Lyatifov, R.B. Materikova and N.S. Kochetkova, J. Organomet. Chem., 169 (1979) 301.
12 B.L. Booth, R.N. Haszeldine and M. Hill, J. Chem. Soc., A, (1969) 1299.
13 T.D. Tilly, R.H. Grubbs and J.E. Bercaw, Organometallics, 3 (1984) 274.
14 W.D. Jones and F.J. Feher, Inorg. Chem., 23 (1984) 2376.
15 F.G.N. Cloke and A.C. Swain, unpublished results.
16 F.G.N. Cloke and J.P. Day, unpublished results.
17 F.G.N. Cloke, J.C. Green, M.L.H. Green and C.P. Morley, J. Chem. Soc., Chem. Commun., (1985) 945.
18 K.A. Asker, A.M. Greenway, K.R. Seddon and A.A. Shimran, J. Organomet. Chem., 354 (1988) 257.
19 A.K. Abdul-Sada, A.M. Greenway and K.R. Seddon, unpublished results.
20 K. Moseley, J.W. Kang and P.M. Maitlis, J. Chem. Soc., A, (1970) 2875.